PHYSICAL REVIEW A **86**, 051605(R) (2012)

Noise- and disorder-resilient optical lattices

Hannes Pichler,[1,2] Johannes Schachenmayer,[1,2,3] Jonathan Simon,[4] Peter Zoller,[1,2] and Andrew J. Daley[3]
[1]*Institute for Theoretical Physics, University of Innsbruck, A-6020 Innsbruck, Austria*
[2]*Institute for Quantum Optics and Quantum Information of the Austrian Academy of Sciences, A-6020 Innsbruck, Austria*
[3]*Department of Physics and Astronomy, University of Pittsburgh, Pittsburgh, Pennsylvania 15260, USA*
[4]*Department of Physics, Harvard University, 17 Oxford Street, Cambridge, Massachusetts 02138, USA*
(Received 7 June 2012; published 16 November 2012)

We show how a dressed lattice scheme can provide control over certain types of noise for atomic quantum gases in the lowest band of an optical lattice, removing the effects of global lattice amplitude noise to first order for particular choices of the dressing field parameters. We investigate the nonequilibrium many-body dynamics of bosons and fermions induced by noise away from this parameter regime, and show how the same technique can reduce spatial disorder in projected lattice potentials.

DOI: 10.1103/PhysRevA.86.051605 PACS number(s): 67.85.Hj, 03.75.Lm, 37.10.Jk, 42.50.−p

Cold atoms in optical lattices provide a unique setting for studying the dynamics of many-body quantum systems based on both control of the microscopic Hubbard Hamiltonian via external fields and isolation of the system from the environment [1–3]. Recent achievements include quantitative studies of equilibrium phase diagrams and phase transitions, and nonequilibrium phenomena such as quench dynamics [4]. Present challenges include realizing the low temperatures or entropies required to see certain fragile many-body phases, for example, in quantum magnetism [4–6] with the relevant energy scale given by the exchange interactions [7–11], and minimizing decoherence sources which can lead to heating. While recent experiments and theoretical studies have identified and investigated spontaneous emission in optical lattices as an example of quantum decoherence [12–14], the heating due to residual (small) laser fluctuations has so far been unexplored. Understanding decoherence associated with such processes involves the study of many-body nonequilibrium dynamics, in which the heating can depend strongly on the form of the many-body state. Though suppression of laser noise or mechanical noise in optical lattice setups is eventually a technological challenge, the more general question is if we can identify lattice setups that are immune against noise in relevant parameter regimes. Below we address these questions for two specific contexts. First, we study the many-body dynamics induced by global laser intensity noise, and propose a setup for a Hubbard model where laser noise is canceled in first order. Second, we show that these ideas can be extended to cancel static spatial disorder in projected optical potentials [15,16], i.e., to *flatten* optical potentials.

We consider noisy optical lattices, in which the potential $V_0(\vec{x}) + \delta V(\vec{x},t)$ fluctuates as $\delta V(\vec{x},t)$, representing either (i) multiplicative time-dependent noise $[\delta V(\vec{x},t) \equiv V_{\text{noise}}(\vec{x})\delta V(t)]$, or (ii) static disorder $[\delta V(\vec{x},t) \equiv \delta V_{\text{dis}}(\vec{x})]$. Below, the corresponding many-body dynamics will be treated for either single-component bosons or two-component fermions, as described by the Hamiltonian ($\hbar \equiv 1$)

$$H_B = \sum_\sigma \int d^3x \hat{\psi}^\dagger_\sigma(\vec{x}) \left[-\frac{\nabla^2}{2m} + V_0(\vec{x}) + \delta V(\vec{x},t) \right] \hat{\psi}_\sigma(\vec{x}) + \sum_{\sigma,\sigma'} \int d^3x d^3x' \hat{\psi}^\dagger_\sigma(\vec{x}) \hat{\psi}^\dagger_{\sigma'}(\vec{x}') U_{\sigma,\sigma'}(\vec{x}-\vec{x}') \hat{\psi}_{\sigma'}(\vec{x}') \hat{\psi}_\sigma(\vec{x}).$$

Here, $\hat{\psi}_\sigma(\vec{x})$ is a bosonic or fermionic field operator with component index σ, m is the particle mass, and $U_{\sigma,\sigma'}(\vec{x}-\vec{x}')$ specifies the two-body interactions.

We aim to identify setups in which the system becomes insensitive to certain types of noise and disorder. We begin with time-dependent noise, where the many-body Hamiltonian can be expressed as $H_B = H_0 + \delta V(t) H_1$, with H_0 specifying the Hamiltonian without the noise, and $\delta V(t)$ the time dependence of fluctuations, which are proportional to H_1. We will show that for some types of noise, a dressed potential can be engineered such that in an effective single-band Hubbard model $[H_0, H_1] = 0$, and the stochastic term can be reinterpreted as a noise on the time parameter of the Schrödinger equation. The system will then be resilient against the noise, e.g., with eigenstates remaining stationary in time and the mean energy of the system remaining constant.

Amplitude noise in an optical lattice. We now specialize to the case of atoms in an optical lattice in the presence of amplitude noise on the lattice depth $V = V_0 + \delta V(t)$, arising from laser intensity fluctuations. This is distinguished, e.g., from mechanical noise on optical elements that can give rise to position shifts of the lattice potential. In experiments, the noise will be associated with a noise spectrum $S_I(\omega) = \int dt \langle \delta V(t) \delta V(0) \rangle e^{i\omega t}$, depending on the technical details of the setup [17]. As depicted in Fig. 1, different components of this noise spectrum will give rise to different dynamical processes. While noise at frequencies of the order of the band separation can give rise to *interband* processes in which particles are transferred to higher Bloch bands, noise at lower frequencies of the order of the tunneling parameter J and on-site interaction strength U will give rise to *intraband* heating for atoms within the lowest band. We note that for relevant frequency scales, intensity fluctuations on the lattice beams give rise to *global* noise on the lattice potential (as the fluctuations are much slower than the time for light to propagate across the system).

When the noise is weak for interband processes (e.g., the spectrum is dominated by $1/f$ low-frequency noise), the evolution of atoms in the lowest Bloch band is governed to first order by a stochastic model for intraband heating (see the Supplemental Material [18] for more details on the validity of

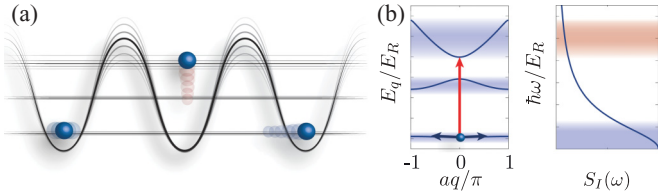

FIG. 1. (Color online) (a) Laser intensity fluctuations give rise to amplitude noise on an optical lattice potential which can produce different heating processes depending on the intensity noise spectrum $S_I(\omega)$. (b) Noise with frequencies of the order of Bloch band separations can give rise to *interband* transitions (red/gray arrow), while processes with frequencies of the order of J and U will give rise to *intraband* heating (blue/dark gray arrows).

this model),

$$i\frac{d|\psi\rangle}{dt} = \left[H(J,U) + H\left(\frac{dJ}{dV},\frac{dU}{dV}\right)\delta V(t)\right]|\psi\rangle, \quad (1)$$

where for bosons $H(J,U)$ is the Bose-Hubbard model

$$H(J,U) = -J\sum_{\langle i,j\rangle} b_i^\dagger b_j + \frac{U}{2}\sum_i b_i^\dagger b_i^\dagger b_i b_i + \sum_i \varepsilon_i b_i^\dagger b_i.$$

The Schrödinger equation (1) describing the dynamics is a multiplicative stochastic differential equation (SDE) [19,20]. Here, b_i is the bosonic annihilation operator for an atom on site i, and the external trapping potential is given by ε_i. We will initially set $\varepsilon_i = 0$, before returning to the trapped case below.

As noted above, the system will be resilient against noise if $H_0 = H(J,U)$ and $H_1 = H(dJ/dV, dU/dV)$ commute. This happens if U/J does not change with the lattice depth, $d(U/J)/dV = 0$, or equivalently

$$\xi \equiv \frac{1}{J}\frac{dJ}{dV} - \frac{1}{U}\frac{dU}{dV} = 0, \quad (2)$$

which defines a *parameter space of sweet spots*. In a typical experimental setup, where the lattice is generated by two counterpropagating beams, we have $dJ/dV < 0$ and $dU/dV > 0$ (and $U, J > 0$) as an increase in the lattice depth increases tunnel barriers and confines the atoms more tightly on each site [3], so that the noise is anticorrelated on J and U. Below we present a lattice setup where the relative noise on J and U can be controlled so that $\xi = 0$. We then analyze in detail the many-body dynamics due to residual heating mechanisms away from $\xi = 0$, arising either from an imperfect implementation of the noise-resilient lattice, or in a typical optical lattice. Finally, we discuss how the the dressed lattice scheme can also be used to remove disorder in projected optical lattices.

Dressed lattice setup to engineer sweet spots. A correlated noise regime with $\xi = 0$ can be obtained with the dressing scheme depicted in Figs. 2(a) and 2(b). We consider two internal atomic states, a primary state $|g\rangle$, trapped in a blue-detuned optical lattice, and an auxilliary state $|h\rangle$, trapped in a red-detuned optical lattice produced by the same laser. This can be achieved, e.g., by tuning the laser in the middle of the fine-structure splitting of an alkali atom [21,22], or by using antimagic wavelength lattices for alkaline-earth atoms [23–25]. The states $|g\rangle$ and $|h\rangle$ are then coupled to produce

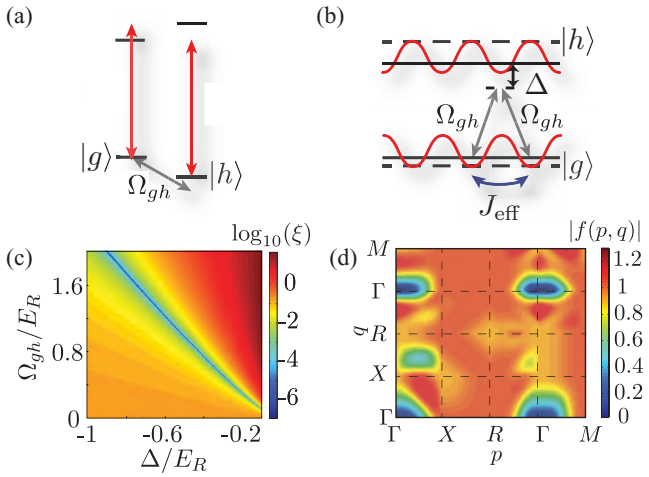

FIG. 2. (Color online) (a) Schematic plot showing coupled internal states used to create dressed lattices for noise or disorder suppression. Two long-lived states $|g\rangle$ and $|h\rangle$ have far-detuned optical lattices created from the same laser (i.e., with identical intensity fluctuations). (b) These internal states are coupled to give rise to a dressed lattice. If the lattice for $|g\rangle$ is blue detuned, and the lattice for $|h\rangle$ red detuned (as indicated by the dashed lines, showing the energy at zero ac-Stark shift), then when the lattice depth increases, the effective detuning decreases, allowing for a larger admixture of $|h\rangle$, and hence an increase in the effective tunneling rate of the dressed atoms. (c) Correlation parameter ξ for different detunings and couplings in an isotropic three-dimensional (3D) lattice of depth $V = 7E_R$ along each dimension. (d) Reduction of disorder, shown as the absolute value of the multiplication factor $|f(p,q)|$ from Eq. (5) for a 3D lattice with $V = 7E_R$, plotted along the lines of symmetry of the first Brillouin zone, i.e., connecting the points $\Gamma = (0,0,0), X = (\pi/a,0,0), R = (\pi/a,\pi/a,\pi/a)$, and $M = (0,\pi/a,\pi/a)$, computed from coupling the lowest Bloch bands.

the dressed lattice. As shown in Fig. 2(b), this coupling (with coupling constant Ω_{gh} and detuning Δ) effectively gives rise to an additional tunneling mechanism for the $|g\rangle$ atoms to move between sites, via a virtual coupling to the state $|h\rangle$. A small increase in lattice depth will shift the effective detuning of this coupling, because the energy levels in the red-detuned lattice shift $\propto -(V + \delta V)$, whereas those in the blue-detuned lattice shift $\propto \sqrt{V + \delta V}$. Thus, if the detuning is chosen appropriately, a small increase in lattice depth can lead to a decrease in the effective detuning, and hence an increase in tunneling due to coupling via the state $|h\rangle$. For an appropriate parameter choice, this will more than compensate for the decrease in bare tunneling for $|g\rangle$, so that $dJ/dV > 0$.

As shown in the Supplemental Material [18], we can always find appropriate values for Ω_{gh} and Δ for typical lattice depths V, and define effective Hubbard model parameters $U_{\rm eff}$ and $J_{\rm eff}$ for the dressed lattice scheme. In Fig. 2(c), we give an example for $V = 7E_R$ (with $E_R = \hbar^2k^2/2m$), plotting ξ as a function of Ω_{gh} and Δ, and demonstrating a line of parameter values where $\xi = 0$ is exactly fulfilled. For any depth, we require $U_{\rm eff} < \Omega_{gh}, \Delta$, but Ω_{gh}, Δ can be comparable to the energy gap between Bloch bands ω. Using larger Δ makes the scheme more robust, e.g., against magnetic field fluctuations that could shift the effective detuning between $|h\rangle$ and $|g\rangle$. We also note that the coupling Ω_{gh} can be produced by an rf

generator for alkali atoms or a clock laser for alkaline-earth atoms [23], which should not add extra noise to the system.

Nonequilibrium stochastic dynamics and heating for correlated and anticorrelated noise. Let us now consider the many-body dynamics away from $\xi = 0$. In the limit of white noise on V, $\langle \delta V(t) \rangle = 0$, $\langle \delta V(t) \delta V(t') \rangle = S\delta(t - t')$, Eq. (1) becomes a Stratonovich SDE [19,20], and we can compute the mean energy increase in the system,

$$\langle \dot{H} \rangle = \frac{S}{2} \left(\frac{1}{J} \frac{dJ}{dV} - \frac{1}{U} \frac{dU}{dV} \right)^2 \langle [[H_J, H_U], H_J] \rangle, \qquad (3)$$

where $H_J = -J \sum_{\langle i,j \rangle} b_i^\dagger b_j$ and $H_U = (U/2) \sum_i b_i^\dagger b_i^\dagger b_i b_i$ denote the kinetic and interaction energy terms in the Bose-Hubbard model. We therefore see that the mean rate of energy increase in this limit grows as ξ^2 away from the sweet spots, and is proportional to the number of particles N (as the commutators are local in space).

It is possible to study many-body dynamics in the presence of noise for varying noise statistics and correlations. We take the example of white noise and propagate Eq. (1) as a many-body SDE using time-dependent density-matrix renormalization group (t-DMRG) methods for a one-dimensional (1D) system [26–29], sampling over noise realizations. We parametrize the correlations between the noise on J and U by θ and λ as $\sqrt{S}(dU/dV)/U = \lambda \sin^2(\theta)$ and $\sqrt{S}(dJ/dV)/J = \lambda \cos^2(\theta)$ for $0 \leqslant \theta < \pi/2$; $\sqrt{S}(dJ/dV)/J = -\lambda \cos^2(\theta)$ for $\pi/2 \leqslant \theta < \pi$. The usual anticorrelated case corresponds to $\theta > \pi/2$, and the sweet spot $\xi = 0$ of Eq. (2) to $\theta = \pi/4$. In Fig. 3(a) we plot the rate of energy increase starting in a Mott insulator (MI) or superfluid (SF) ground state as a function of θ, keeping the sum of the relative noise on J and U terms constant. In agreement with Eq. (3), we observe that for anticorrelated noise ($\theta > \pi/2$), the rate of energy increase depends only on S, and not on θ, whereas for correlated noise ($\theta < \pi/2$) we observe a quadratic increase in the heating rate around the sweet spot. The effects of classical noise are significant for both MI and SF states.

In Fig. 3(a) we also show the heating in the presence of a harmonic trapping potential originating from a slowly varying mean intensity of the lattice (with corresponding noise). When such a trapping potential is included in H_0, it is no longer possible to fulfill the condition $[H_0, H_1] = 0$ exactly. However, for typical values of the trapping frequencies the residual heating is extremely small at $\xi = 0$, and in Fig. 3(a) is over two orders of magnitude smaller than for anticorrelated noise.

For the Mott insulator state, the noise produces correlated particle-hole pairs that spread through the system as a function of time. This is shown in Fig. 3(b), where we plot parity-parity correlation functions $\mathcal{C}_k(t) = \langle \hat{s}_l \hat{s}_{l+k} \rangle - \langle \hat{s}_l \rangle \langle s_{l+k} \rangle$ with $\hat{s}_l = \exp[i\pi(\hat{n}_l - 1)]$, which can be measured in experiments with a quantum gas microscope [30,31]. Initially, the nearest-neighbor parity-parity correlations are strongest, resulting from virtual tunneling of particles to neighboring sites with an amplitude J/U. The amplitude noise produces real particle-hole excitations, which transfer initially to next-neighbor sites and then spread through the system, while the nearest-neighbor correlation functions decrease monotonically, as shown in Fig. 3(c). For weakly interacting superfluid states, the heating is traced to creation of pairs of Bogoliubov excitations, leading to a decrease in the condensate fraction [32], and energy

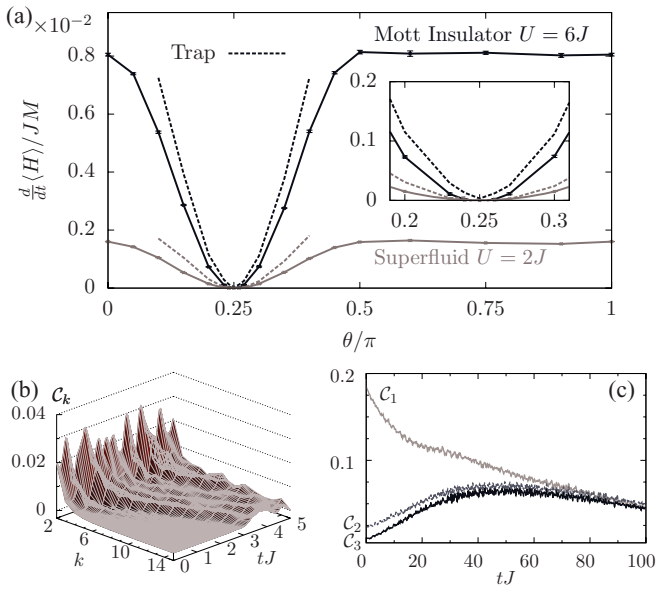

FIG. 3. (Color online) (a) Short-time ($tJ \leqslant 2$) heating rates of superfluid ($U = 2J$) and Mott insulator states ($U = 6J$) in 1D as a function of the relative magnitude of noise on J and U, θ. Results are from linear regression over 500 t-DMRG trajectories in a system with $M = 30$ sites and $N = 30$ particles with open boundary conditions. In both cases heating is strongly suppressed in the vicinity of the sweet spot at $\theta \sim 0.25\pi$ (expanded in the inset). Dashed lines show results in the presence of a harmonic trap with $\varepsilon_i/J = 0.0356i^2$, $\sqrt{S}(d\varepsilon_i/dV)/\varepsilon_i = 5 \times 10^{-3} J^{-1/2}$, and $N = 30$ (t-DMRG bond dimension $D = 100$). (b), (c) The effect of amplitude noise on parity-parity correlations on an initial Mott insulator state ($U = 6J$), with anticorrelated noise $\theta = 0.75\pi$. (b) Short-time evolution for a single noise trajectory with $M = 30$ (t-DMRG bond dimension $D = 200$). (c) Long-time evolution of these correlations calculated for $M = 10$ sites averaged over 1000 noise trajectories. (For all parts, $\lambda = 0.02 J^{-1/2}$, time step $\Delta t = 10^{-2}/J$.)

increase per particle at a rate $\dot{E}/N \approx S\xi^2 z J U^2 \bar{n}$, where z is the number of nearest neighbors and $\bar{n}$ is the filling factor.

We observe similar behavior for a Fermi Hubbard model,

$$H_{\mathrm{FH}} = -J \sum_{\langle i,j \rangle} c_{i,\sigma}^\dagger c_{j,\sigma} + U \sum_i c_{i\uparrow}^\dagger c_{i\uparrow} c_{i,\downarrow}^\dagger c_{i,\downarrow}, \qquad (4)$$

where $c_{i,\sigma}$ is a fermionic annihilation operator for a particle in state $\sigma \in \{\uparrow, \downarrow\}$ on site i. In Fig. 4 we plot a similar analysis to Fig. 3(a), beginning in the ground state for $U \ll J$ at half filling, where the state exhibits antiferromagnetic order [7] (which in 1D is characterized by algebraically decaying antiferromagnetic correlations). The heating mechanism here involves excitations above the underlying Mott insulator state, and we again see that the noise here is also robustly suppressed around the sweet spot, as in the bosonic case. In a mean-field approximation, the heating rate per particle is given by $\dot{E}/N \approx S\xi^2 U z J^2$.

Removal of spatial disorder. Another application of the dressed lattices is to flatten spatial disorder as it arises in projected lattices [15,16] and other slowly varying, shallow potentials, by choosing Δ and Ω_{gh} such that $d\varepsilon_{\mathrm{eff}}/dV = 0$. While disorder is interesting in its own right [33,34], in projected lattice setups it arises as spatial intensity variations

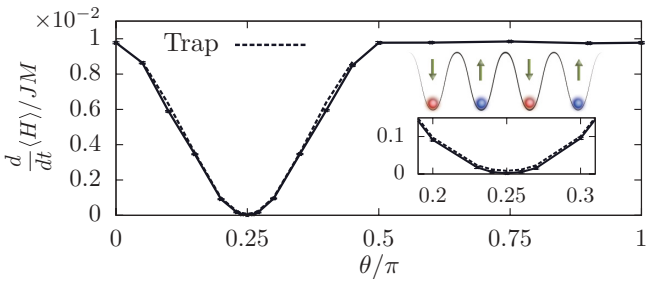

FIG. 4. (Color online) Heating rates around the sweet spot for a two-species Fermi-Hubbard model in 1D, with an initial antiferromagnetic ground state with interspecies interaction $U = 10J$. The noise is parametrized as in Fig. 3. The solid lines show a system with $M = 30$, and 15 particles of each species, the dashed lines a trapped case with $\varepsilon_i/J = 0.015i^2$, and 20 particles of each species.

due to imperfections in the imaging system, and is a challenge for producing homogeneous trap regions. If we transform the Hamiltonian into a quasimomentum representation, then by considering the coupling between the lowest bands in the lattice for $|g\rangle$ and $|h\rangle$ we can show that the disorder Hamiltonian $H_D = \sum_{p,q} \delta\varepsilon_g(q) a^\dagger_{p+q,g} a_{p,g}$ (where $a_{p,\sigma}$ is a bosonic annihilation operator for a particle with internal state σ and quasimomentum p) becomes an effective disorder in the dressed lattice

$$H_D \to \sum_{p,q} \delta\varepsilon_g(q) f(p,q) a^\dagger_{p+q,-} a_{p,-}, \tag{5}$$

with $\sigma = -$ indicating the lower-energy dressed state. That is, the "disorder" is multiplied by the factor $f(p,q)$. In Fig. 2(d) we show $|f(p,q)|$ computed for an isotropic 3D lattice, and plotted along the lines of symmetry in the Brillouin zone. The suppression works well for disorder varying slowly on the scale of a lattice site, i.e., $|q|$ is not too large, or if the quasimomentum of the state $|p|$ is not too large. For disorder of the scale of two sites, there is a reduction of the disorder by a factor greater than 2, and for the small quasimomentum states that are typically most affected by the disorder potential, the reduction can be more than an order of magnitude.

Summary and outlook. We have presented a dressing scheme that can be used to suppress either amplitude noise or disorder arising from spatial intensity fluctuations for atoms in the lowest band of an optical lattice. This scheme works for bosons and fermions, and could be used as a tool for studies of nonequilibrium many-body dynamics driven by noise [35,36].

We thank S. Blatt, M. Lukin, and the groups of I. Bloch and W. Ketterle for helpful and motivating discussions. This work was supported in part by the Austrian Science Fund through SFB F40 FOQUS, by AFOSR Grant No. FA9550-12-1-0057, and by a grant from the US Army Research Office with funding from the DARPA OLE program. Work in Innsbruck is supported by the integrated project AQUTE. Computational resources were provided by the Center for Simulation and Modeling at the University of Pittsburgh.

[1] I. Bloch, J. Dalibard, and W. Zwerger, Rev. Mod. Phys. **80**, 885 (2008).
[2] M. Lewenstein, A. Sanpera, V. Ahufinger, B. Damski, A. Sen, and U. Sen, Adv. Phys. **56**, 243 (2007).
[3] D. Jaksch and P. Zoller, Ann. Phys. **315**, 52 (2005).
[4] J. I. Cirac and P. Zoller, Nat. Phys. **8**, 264 (2012); I. Bloch, J. Dalibard, and S. Nascimbène, *ibid.* **8**, 267 (2012).
[5] U. Schneider, L. Hackermüller, S. Will, Th. Best, I. Bloch, T. A. Costi, R. W. Helmes, D. Rasch, and A. Rosch, Science **322**, 1520 (2008).
[6] R. Jördens, N. Strohmaier, K. Günter, H. Moritz, and T. Esslinger, Nature (London) **455**, 204 (2008).
[7] R. Jördens, L. Tarruell, D. Greif, T. Uehlinger, N. Strohmaier, H. Moritz, T. Esslinger, L. De Leo, C. Kollath, A. Georges, V. Scarola, L. Pollet, E. Burovski, E. Kozik, and M. Troyer, Phys. Rev. Lett. **104**, 180401 (2010).
[8] D. M. Weld, P. Medley, H. Miyake, D. Hucul, D. E. Pritchard, and W. Ketterle, Phys. Rev. Lett. **103**, 245301 (2009).
[9] P. Medley, D. M. Weld, H. Miyake, D. E. Pritchard, and W. Ketterle, Phys. Rev. Lett. **106**, 195301 (2011).
[10] D. McKay and B. DeMarco, New J. Phys. **12**, 055013 (2010).
[11] D. McKay and B. DeMarco, Rep. Prog. Phys. **74**, 054401 (2011).
[12] H. Pichler, A. J. Daley, and P. Zoller, Phys. Rev. A **82**, 063605 (2010).
[13] S. Trotzky, L. Pollet, F. Gerbier, U. Schnorrberger, I. Bloch, N. Prokofiev, B. Svistunov, and M. Troyer, Nat. Phys. **6**, 998 (2010).
[14] F. Gerbier and Y. Castin, Phys. Rev. A **82**, 013615 (2010).
[15] W. S. Bakr, J. I. Gillen, A. Peng, S. Fölling, and M. Greiner, Nature (London) **462**, 74 (2009).
[16] J. Simon, W. S. Bakr, R. Ma, M. E. Tai, P. M. Preiss, and M. Greiner, Nature (London) **472**, 7343 (2011).
[17] See, e.g., A. Liem, J. Limpert, H. Zellmer, and A. Tünnermann, Opt. Lett. **28**, 1537 (2003).
[18] See Supplemental Material at http://link.aps.org/supplemental/10.1103/PhysRevA.86.051605 for a derivation of the Stochastic Hubbard Model in the instantaneous frame, details of the noise-resilient setup and an analysis of the effects of fluctuations of the coupling fields in this setup.
[19] P. E. Koeden and P. Platen, *Numerical Solution of Stochastic Differential Equations*, Springer Series in Stochastic Modelling and Applied Probability Vol. 23 (Springer, Berlin, 1992).
[20] C. Gardiner, *Stochastic Methods*, Springer Series in Synergetics (Springer, Berlin, 2009).
[21] D. Jaksch, H.-J. Briegel, J. I. Cirac, C. W. Gardiner, and P. Zoller, Phys. Rev. Lett. **82**, 1975 (1999).
[22] O. Mandel, M. Greiner, A. Widera, T. Rom, T. W. Hänsch, and I. Bloch, Phys. Rev. Lett. **91**, 010407 (2003).
[23] J. Ye, H. J. Kimble, and H. Katori, Science **320**, 1734 (2008).
[24] W. Yi, A. J. Daley, G. Pupillo, and P. Zoller, New J. Phys. **10**, 073015 (2008).
[25] A. J. Daley, M. M. Boyd, J. Ye, and P. Zoller, Phys. Rev. Lett. **101**, 170504 (2008).

[26] G. Vidal, Phys. Rev. Lett. **93**, 040502 (2004).
[27] A. J. Daley, C. Kollath, U. Schollwöck, and G. Vidal, J. Stat. Mech.: Theor. Exp. (2004) P04005.
[28] S. R. White and A. E. Feiguin, Phys. Rev. Lett. **93**, 076401 (2004).
[29] F. Verstraete, V. Murg, and J. I. Cirac, Adv. Phys. **57**, 143 (2008).
[30] M. Cheneau, P. Barmettler, D. Poletti, M. Endres, P. Schauß, T. Fukuhara, C. Gross, I. Bloch, C. Kollath, and S. Kuhr, Nature (London) **481**, 484 (2012).
[31] P. Barmettler, D. Poletti, M. Cheneau, and C. Kollath, Phys. Rev. A **85**, 053625 (2012).
[32] H. Pichler, J. Schachenmayer, A. J. Daley, and P. Zoller (unpublished).
[33] B. Deissler, M. Zaccanti, G. Roati, C. D'Errico, M. Fattori, M. Modugno, G. Modugno, and M. Inguscio, Nat. Phys. **6**, 354 (2010).
[34] F. Jendrzejewski, A. Bernard, K. Mueller, P. Cheinet, V. Josse, M. Piraud, L. Pezzé, L. Sanchez-Palencia, A. Aspect, and P. Bouyer, Nat. Phys. **8**, 398 (2012).
[35] E. G. D. Torre, E. Demler, T. Giamarchi, and E. Altman, Nat. Phys. **6**, 806 (2010).
[36] G. Bunin, L. D'Alessio, Y. Kafri, and A. Polkovnikov, Nat. Phys. **7**, 913 (2011).